Electrical Resistance Rheometry – The Application of Multi-scale Tomography Sensors to Provide in-pipe Rheology in Complex Processes

Thomas D. Machin[1,2*], K. Wei[2], R.W. Greenwood[1], M.J.H Simmons[1]

[1]University of Birmingham, Birmingham, UK
[2]Industrial Tomography Systems PLC, Manchester, UK

[*]Email: tom.machin@itoms.com

ABSTRACT

The rheology of a fluid system is a vital property in a wide range of physical and chemical industrial processes as it governs process quality and efficiency. Conventionally, rheological properties are measured off-line with the removal of a sample from the process stream required. Off-line measurements are applied to flows within real processes; however, the majority of attempts have been unsatisfactory as it only offers a retrospective characterisation. Accordingly, there is an ever-increasing demand for the development of in-line rheometers as most industrial fluids exhibit complex rheological behaviour. A novel, in-line Electrical Resistance Rheometry technique is outlined in this paper which utilises a combination of multi-scalar microelectrical tomography sensors to perform in-situ measurements on process fluids. By cross-correlating fluctuations of computed conductivity pixels across and along a pipe, the rheological behaviour of a fluid is able to be obtained directly through the measurement of the velocity profile. The measurement of a flow profile with Electrical Tomography is well-established; however, the resolution in the near-wall region of the pipe has limited its application to monitor rheology. This has been overcome with the inclusion of multi-scalar arrays permit the specific targeting of the electrical field to a desired region of interest, in this instance near to the pipe-wall. Across a range of well characterised materials, the measured velocity profile and extracted rheological parameters have been verified with Particle Image Velocimetry and rotational rheometry, respectively. The manipulation of array length, and consequently electrical field penetration, has been utilised for the first time within this study and has further applications in other unit operations, for example stirred tanks.

Keywords multi-scaled sensing, in-line, rheology, process optimisation

Industrial Application General

1 INTRODUCTION

The rheological properties of a fluid system are critical in chemical and physical processing, since they govern both in-process efficiency and final product quality. Conventionally, off-line measurements of such properties or required to extract such information careful sampling and removal from the product stream. The fluid rheology obtained from such measurements is often considered, without assumptions, as applicable to real process flows. However, the application of off-line measurements is in the majority unsatisfactory since such an approach only permits a retrospective characterisation of the sample structure which may not be representative of structure as a function of the time-shear history received during processing. In-situ measurements are able to overcome this deficiency as they are inherently conducted within the flow environment and remove the possibility of degradation of the sample. Since in-line rheometery measurements are conducted within the process flow environment, they possess the capability to elevate rheometry from a quality control tool at process end-point to one which is able to control and optimise processes. Despite this, the currently exists no commercially viable technique has been outlined which is capable of performing this task efficiently across a wide range of fluids (Rees, 2014).

In alignment with this demand, numerous studies have been undertaked to uncover in-pipe, in-line properties of rheology with a particular focus upon ultrasound Doppler-based velocity profiling (UVP)

techniques (Wiklund et al, 2007). Despite some positive results, UVP is only applicable to systems which contain particles acting as tracers or to the velocity measurement of the dispersed phase in a two-phase flow system (Dong et al, 2016). As a result, the applications of this technique are limited with several setups and studies reporting UVP is prone to several sources of correlated and uncorrelated noise (Wiklund et al, 2007). Furthermore, UVP cannot be applied successfully in aerated systems, greatly limiting its in-plant applicability.

The robust nature, wide-ranging applicability and simple implementation of microelectrical tomography sensors to industrial processing provides an ideal basis for the development of an in-line rheometer. The application of such sensors to in-pipe rheometry was termed Electrical Resistance Rheometry (ERR) by Machin et al (2018). Sharifi and Young (2013) utilised a step change in saline solution concentration to monitor the motion of across two planes of circular ERT sensors using AIMFLOW software, developed by Industrial Tomography Systems; however, the acquired velocity measurements did not capture the velocity profile effectively due to a lack of sensitivity in the pipe-wall boundary region. To ensure a complete velocity profile is attained, Machin et al (2018) developed a novel, in-line ERR sensor configuration which utilised a multi-scaled approach utilising a combination of electrical resistance sensor types, multi-scalar and circular arrays.

The novel sensor setup utilises a multi-scaled approach in order to target sensitivity of the electrical field to a region of interest. The manipulation of the multi-scalar, or linear, array length, and consequently electrical field penetration, has been utilised for the first time in development of Electrical Resistance Rheometry; this provides an opportunity for the development of a number of electrical resistance sensing techniques.

2 MULTI-SCALE ELECTRICAL RESISTANCE SENSING

Linear ERT sensor configurations have become well-established since they were first developed by Qui et al (1994) for the imaging of sub-seabed porosity. This arrangement consists of an array of coplanar strip electrodes and has numerous industrial applications with a particular focus upon developing an understanding of axial mixing in agitated vessels. However, a novel application of this arrangement is to act as a multi-scale sensor, which is capable of targeting the electrical field penetration based upon the sensor size.

If a current is applied to two similar coplanar parallel conducting strips, the potential distribution is approximately elliptical in shape (Smythe, 1968). As the distance between the plates increases, the radius of this ellipse increases accordingly and hence does the electrical field penetration into the fluid. A COMSOL model demonstrating the electrical field distribution is displayed in Figure 1 for a fluid, of conductivity 1 mS cm^{-1} and relative permittivity of 5 for multi-scalar arrays of length 15 mm and 25 mm. In both cases, an alternating current excitation signal which possessed a current of 1 A and frequency of 19200 Hz; these simulations were also performed at 20 °C. The model neglects induction, assumes that the electrical field is curl free, consequently, this model is derived from Maxwell's equations, Eqs 1, 2 and 3. Maxwell's equations govern the mathematical formulation of Electrical Impedance Tomography (Wang, 2015).

$$-\nabla\big((\sigma + j\omega\varepsilon_r\varepsilon_0)\nabla V\big) = 0 \tag{1}$$

where σ is the electrical conductivity, in S m^{-1}, ϵ_r and ϵ_0 are the relative permittivity and permittivity of free space, in F m^{-1}, respectively.

$$\mathrm{E} = -\nabla \mathrm{V} \tag{2}$$

$$\mathrm{D} = \varepsilon_\mathrm{r}\varepsilon_0\mathrm{E} \tag{3}$$

where the electric field, E and displacement, D, are obtained from the electric field gradient V

From this simulation, it can be observed that the concentration of electrical field lines for the array of 15 mm is confined relatively close to the electrodes with a penetration depth of approximately 5 mm. However, when the multi-scalar array size increases to 25 mm this electrical field is capable of penetrating further into the fluid to a distance of 9 mm. This behaviour may be exploited in the design

of novel sensors to interrogate desired regions of interest and perform conventional ERT measurements in such regions.

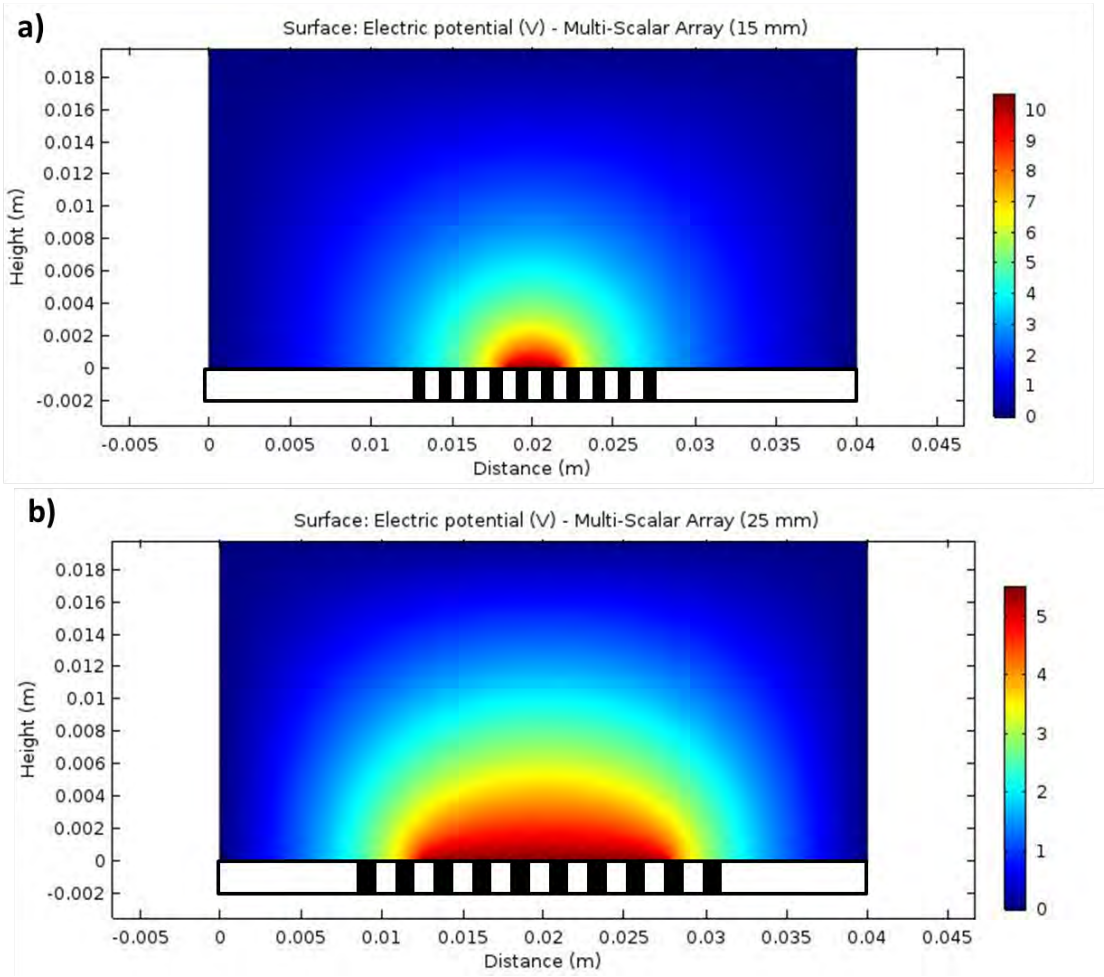

Figure 1. Electrical Field Penetration for multi-scale arrays (a) 15 mm array, (b) 25 mm array

It is known that the conductivity of the fluid impacts upon the electrical field penetration with an increase in conductivity reducing the confinement of the electrical field. Despite this, the Industrial Tomography Systems plc (ITS) v5r system is a voltage driven measurement, which adjusts the applied current according to the fluid being interrogated and consequently, a constant electrical field penetration is retained. Hence the ITS v5r instrument is able to facilitate a vast number of sensing opportunities to target regions of interest across a wide range of unit operations, by simply manipulating the geometry of a sensor.

3 ELECTRICAL RESISTANCE RHEOMETRY: THE CONCEPT

3.1 Velocity Profile Extraction

Electrical Resistance Rheometry (ERR), developed by Machin et al (2018) affords rheological characterisation via the measurement of the radial velocity profile to elucidate the shear rate profile within a pipe. The cross-correlation algorithm is employed to monitor the fluctuations in computed conductivity pixels of a reconstructed tomogram, Eq. 4; this tags the motion of a fluid across and within multiple measurement planes (Papoulis, 1962). As the measurement geometry is fixed, the extracted time delay may be converted to velocity.

$$R_{12}(\tau) = \int_{-\infty}^{\infty} f(t)g(t-\tau)dt \quad (4)$$

where R_{12} is the cross correlation function; τ is the displacement between the two continuous functions, in seconds and f(t) and g(t) are continuous conductivity functions as a function of time.

The Electrical Resistance Rheometer utilises four arrays of eight electrodes, consisting of two multi-scalar arrays and two circular arrays resulting in the output of four tomograms. This arrangement is operated using the ITS v5r system which is capable to operate a sensor consisting of a maximum of 32 electrodes. Linear, or multi-scalar, array measurements are reconstructed to rectangular tomograms which comprise of 10 x 20 pixels and circular tomograms consisting of 316 pixels, this is displayed in Figure 2b. The inclusion of such circular sensors additionally permits the visualisation of the cross-sectional impedance map to simultaneously interrogate localised and global mixing behaviour in-line.

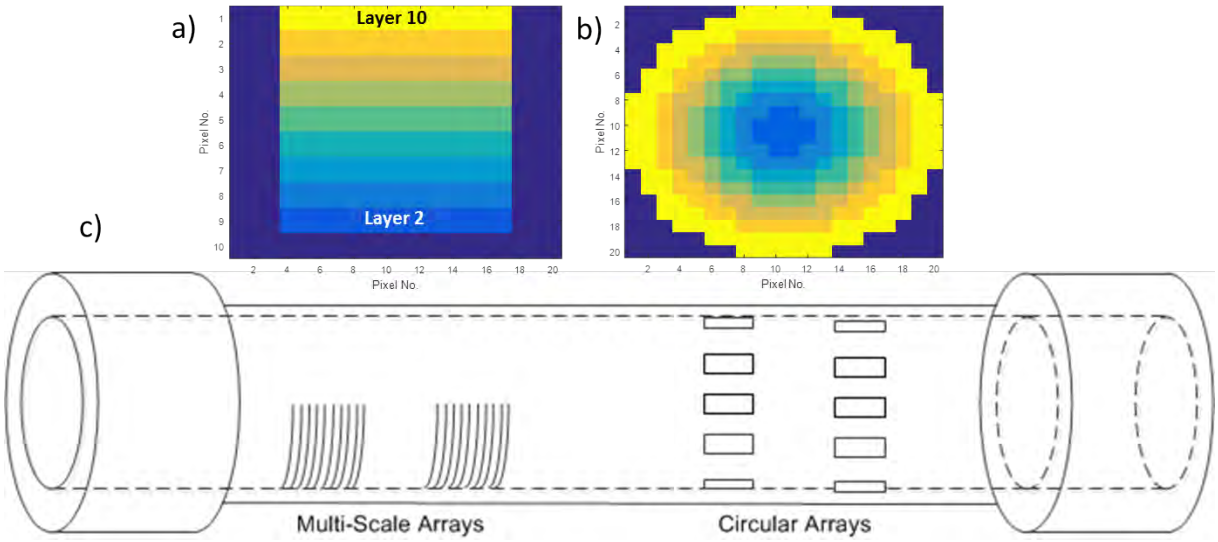

Figure 2. Electrical Resistance Rheometry Sensor (Machin et al, 2018) a) Multi-scale array zone scheme, b) Circular array zone scheme, c) Electrical Resistance Rheometry sensor

The tomograms may be segmented to develop a number of radial velocity measurement positions in the pipe. The bottom layer of pixels in the multi-scale tomograms were removed alongside the first and last three pixels, in the direction of flow to reduce noise. This condenses the tomogram from 10 x 20 pixels to 9 x 14 pixels; each of the 9 layers each form a radial measurement point, Figure 2a. These nine measurements may then been further reduced to four, via averaging, to introduce an 'effective' weighting. As a result, a greater number of measurement points are located in the central pipe region which is associated with low shear rates, whilst ensuring a complete velocity profile is obtained. Similarly, the circular tomogram has been separated into eight zones based upon radial position. The obtained conductivity in each of these zones is averaged, normalised and with the cross-correlation algorithm subsequently performed across and within measurement arrays.

A pulsed ohmic heater (C-Tech Innovation, UK) was developed as a conductivity perturbation to deliver a small, short rise in temperature and conductivity. Ohmic heating imparts an alternating current, and hence electrical energy, to the fluid which is converted to thermal energy uniformly across the entire pipe cross-section (Knirsch et al, 2010).

3.2 Rheology Extraction

A fluid's rheological properties influence the velocity profile shape in laminar pipe flow due to a shear rate response. Accordingly, the raw velocity measurements may act as a fingerprinting tool; this can be used to infer rheological behaviour of complex fluids systems. However, If the rheological behaviour adheres to conventional rheological models, the velocity profile can be related to the constitutive equation of the fluid and directly output the desired parameters. The specific constitutive equation for a power law fluid is given as:

$$\tau = k\dot{\gamma}^n = k\left(-\frac{du}{dr}\right)^n \quad (5)$$

where τ is shear stress, in Pa; k is consistency index, in Pa s^n; $\dot{\gamma}$ is shear rate, in s^{-1}, n is consistency index; u is velocity within the pipe, in m s^{-1}, and r is radius, in m.

The velocity profile may then be coupled with the measurement of differential pressure to obtain the shear stress profile (Wilkinson, 1960).

$$T = \frac{\Delta P \cdot r}{2L} \quad (6)$$

where ΔP is the differential pressure drop, in Pa, along a pipe length, L, in m, with r representing a pipe radius, in m.

Substituting Eq. 5 into Eq. 6 with subsequent re-arrangement and integration, implementing the boundary conditions of u = 0 at r = R and u = u at r = r, yields the velocity profile for a power law fluid.

$$u(r) = \left(\frac{\Delta P}{2kL}\right)^{\frac{1}{n}}\left(\frac{n}{n+1}\right)\left(R^{\frac{n+1}{n}} - r^{\frac{n+1}{n}}\right) \quad (7)$$

A parametric fitting of the ERR velocity profile to the theoretical velocity profile may then be employed to extract rheological parameters; the Levenberg-Marquadt algorithm was employed (Marquadt, 1968). As this algorithm does not contain second derivatives the computational time is reduced affording high temporal resolution.

4 METHODOLOGY

4.1 Materials

Three aqueous-based fluids were selected for experimentation: glycerol (Darrant Chemicals, UK); xanthan gum, from Xanthomonas Campestris (Sigma-Aldrich, UK) and Carbopol 940 (Lubrizol, UK). These fluids typically adhere to common rheological constitutive equations.

These test fluids consisted of 75 wt%, 85 wt% and 92.5 wt% aqueous glycerol and 0.1 wt%, 0.5 wt% and 1.0 wt% xanthan gum powder dissolved in water to form solutions which observe Newtonian and shear thinning power law behaviour, respectively. Two Carbopol formulations were selected for this study, 0.1 wt% Carbopol, pH 7 and 1.0 wt% Carbopol, pH 7. The pH of the Carbopol solutions was amended by including 0.1 M Sodium Hydroxide (Sigma-Aldrich, UK) to generate a gel matrix which may be described using the Herschel-Bulkley model (Simmons et al, 2009).

The fluid's rheology were extracted using an AG R2 rotational rheometer (TA Instruments) equipped with a smooth-walled, 4.006° stainless steel cone and plate geometry of diameter 40 mm. The sample was held at 23 ± 0.1°C using an Peltier plate, before a logarithmic shear rate ramp was applied across the shear rate range of 0.01 - 1500 s-1, over a duration of 600 seconds with 20 points per decade. To extract fitted rheological parameters, a non-linear least squares regression was applied in the TRIOS software, (TA instruments). The resultant rheological properties acquired are presented in Table 1.

4.2 Electrical Resistance Rheometry

A recirculating pipeline was setup, Figure 3, which consisted of an 60 L vessel and a controlled positive displacement pump (Fristam Ltd., UK) operated by a personal computer. The 1-inch inner diameter ERR sensor was located in-line with the ohmic heater. The measurement of differential pressure was performed across the length of both the ohmic heater and ERR sensor and recorded alongside flow rate and temperature. The flow rate was monitored using a micro motion Coriolis flow meter (Emerson Ltd., UK).

The experimental fluids were examined across the flow rate range of 40 – 350 L hr^{-1}, with the ERR sensor and operated by a v5r ERT instrument (ITS, UK). The 4 planes, of 8 electrodes configuration

was utilised alongside the adjacent electrode measurement protocol. The sensor was operated with two multi-scalar arrays, of length 12 mm, and two circular arrays. The v5r was operated in block mode with one sample delay cycle to enable a frame rate of 325 frames per second. For a single measurement 12,000 frames were captured to monitor the conductivity perturbation generated by the ohmic heater, whose voltage injection was set in the range of 1 – 1.5 kV for 0.5 – 1 s.

The obtained raw data was fed into a MATLAB code which contained the Modified Standard Back projection reconstruction algorithm (Wang, 2002) and subsequent rheological analysis.

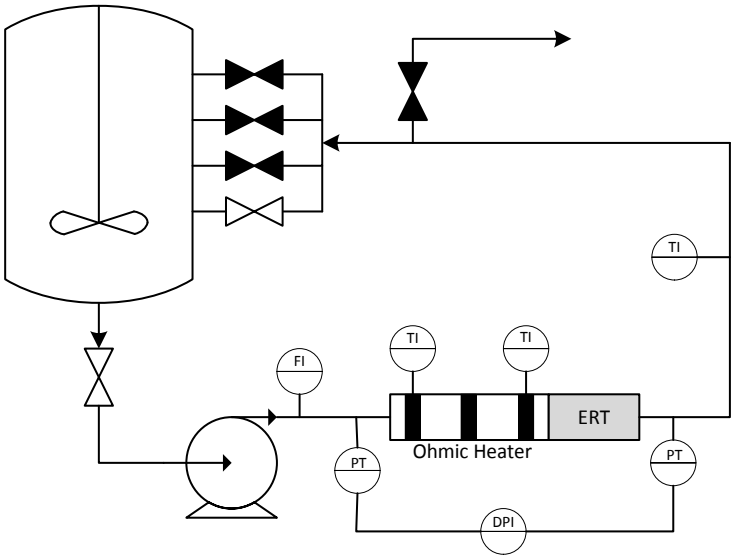

Figure 3. Experimental flow loop setup schematic (Machin et al, 2018)

4.3 Particle Image Velocimetry (PIV)

2-D PIV measurements were performed to validate the ERR velocity profile; which were achieved using a TSI PIV system. A 532 nm (green) laser (Litron Nano PIV), pulsed at 7 Hz, was synchronised to a single TSI Power view 4MP 12 bit CCD camera using a synchroniser operated by a personal computer. The TSI Insight 4G software was utilised to control the experiment, process data and generate velocity fields with subsequent radial velocity profile measurement averaging performed in MATLAB. The Nyquist PIV algorithm was used to obtain these velocity fields.

PIV measurements were conducted within a circulation loop without the inclusion of the ohmic heater to determine its effect upon the measured velocity profile. For each flow rate, 500 images were captured with average flow field determined. The spatial resolution of this setup was 12 μm pixel^{-1} with an interrogation area of 64 x 64 pixels and the Gaussian peak method applied. It must be acknowledged that 1.0 wt% xanthan gum was unable to be interrogated due to its opaque nature.

5 RESULTS AND DISCUSSION

5.1 Penetration Factor

Preliminary experiments were performed to validate the radial positioning for each of the multi-scalar array tomogram zones. The conductivity of an aqueous glycerol solution, 75 wt%, was varied from 0.025 - 10 mS cm^{-1}, with the acquired multi-scale velocity profile measured. As glycerol is known to exhibit Newtonian properties and observe a parabolic velocity profile, the measured velocity points were fitted to the theoretical velocity profile to determine the electrical field penetration, with the results displayed in Figure 4. A penetration factor may then be derived, Eq. 8. Once obtained, this electrical field penetration depth is kept constant throughout all experiments.

$$\text{Pentration Factor} = \frac{\text{Optimised Radius}}{\text{Sensor Length}} \tag{8}$$

As the ITS v5r ERT instrument is a voltage driven measurement, with the amplitude of the applied current is varied during the measurement depending upon the fluid conductivity observed. Therefore, the penetration factor should remain constant irrespective of fluid conductivity. This behaviour is depicted in Figure 4b.

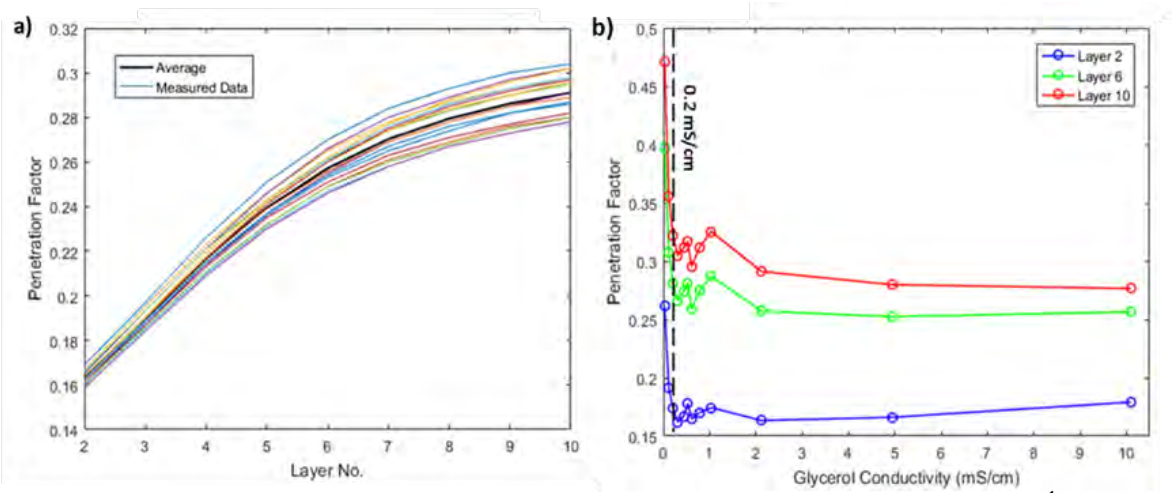

Figure 4. Penetration Factor a) Penetration factor for a 75 wt% glycerol solution of conductivity 2 mS cm^{-1}, b) variation in penetration factor with conductivity

For all glycerol solution conductivities, the penetration was seen to repeatedly be of parabolic nature, with the largest variations observed at the largest radial distance away from the pipe wall. At this point, for an array length of 12 mm the physical variation in electrical field penetration is only approximately 0.5 mm. When altering the conductivity, below 0.2 mS cm^{-1} an increase in the penetration factor is observed; however, above this point it plateaus to a constant value of 0.3 for the layer furthest away from the wall. It can therefore be said that multi-scalar sensors alongside the v5r are operate at constant penetration depth for the conductivity of 0.2 – 10 mS cm^{-1} and is expected to operate at much higher conductivities as the ITS v5r is amenable to higher conductivities up to 200 mS cm^{-1}.

5.2 Velocity Profile Extraction

Critical to the in-situ determination of rheology, the velocity profile must first be interrogated with the obtained results displayed in Figure 5. It is evident that the Newtonian glycerol solutions observe the conventional parabolic velocity profile of laminar pipe flow, Figure 5a. When changing the fluid to the shear-thinning, xanthan gum solutions, the shear rate response increases the blunting of the parabolic velocity profile with increased xanthan gum concentration. The flattening of the velocity profile is indicative of shear-thinning behaviour and is illustrated in Figure 5b. It can also be observed that for a 1.0 wt% xanthan gum solution the obtained velocity profile observes increased flattening, and hence degree of shear-thinning, in comparison to the 0.5 wt% xanthan gum solution, despite the former conducted at a greater flow rate.

A similar shape is observed during the extraction of Carbopol 940 solutions, which was modelled as a Herschel-Bulkley fluid, with a flat region indicative of a plug flow and the presence of a yield stress. As the flow rate increases, the radius of the plug is reduced signifying that the yield stress is being tracked; this is due to the increased magnitude of the opposing shear stress at an increased flow rate. Moreover, a comparison of two Carbopol concentrations observes a large difference in the length of the velocity profile plug region which demonstrates the higher yield stress of the more concentrated 1.0 wt% Carbopol, pH 7 solution. Consequently, it could therefore be stipulated that the ERR velocity profiles match the experimented upon theoretical velocity profiles and demonstrate repeatability throughout with minor variations of the velocity profile observed at a constant flow rate. The acquired velocity profiles for the 1.0 wt% Carbopol solution pH 7, is displayed in Figure 5c.

To quantify these results, a statistical analysis has been performed across 20 independent ERR velocity profiles at every radial velocity position. This gives rise to an average 95 % confidence interval of ± 2.93 % when compared to the mean. This variation yields as a mean standard error in velocity of just 0.0043 m s^{-1} which is seen to be similar across all radial positions. Resultantly, measurement points located near the wall observe a greater uncertainty; however, this is dampened in the

parametric fitting due to an 'effective' weighting with more radial velocity measurement at the centre of the pipe. The radial velocity profile obtained by ERR may be considered to be in close agreement with the theoretical laminar velocity profile with a typical correlation coefficient, R^2, of 0.99 between raw and accepted velocity values which additionally lie within one standard error of one another.

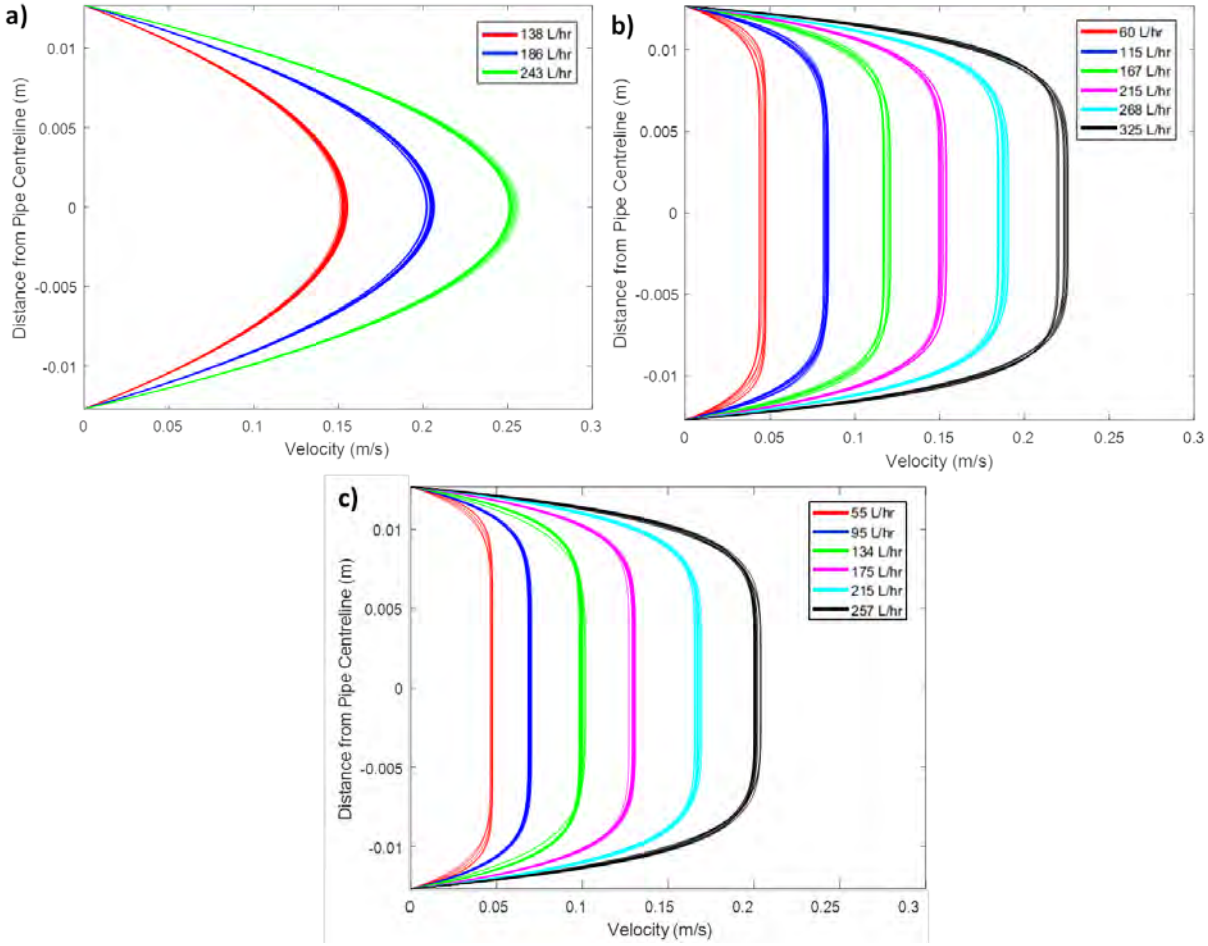

Figure 5. Electrical Resistance Rheometry Velocity Profiles: (a) 75 wt% glycerol – multiple flow rates; (b) 1.0 wt% xanthan gum – multiple flow rates; (c) 1.0 wt% Carbopol, pH 7 – multiple flow rates.

5.3 Particle Image Velocimetry (PIV)

PIV permits Electrical Resistance Rheometry and the multi-scale sensing approach to be validated against a widely accepted and extensively studied velocimetry technique of superior spatial resolution. The obtained results from 75 wt% glycerol at a flow rate of 240 L hr^{-1} are displayed in Figure 6b and 6c alongside an example capture, Figure 6a, with the anticipated parabolic velocity profile observed. Comparing ERR with the PIV measurement a residual sum of squares of 4.43×10^{-4} m^2 s^{-2} exists and a correlation coefficient of 0.9992. Consequently, the measured glycerol velocity profiles can be said to be parabolic.

This provides a vital result as the irrotational flow regime has been achieved due to the removal of hydrodynamic entrance effects; this affords the application of laminar flow theory. To achieve irrotational flow, an entrance length, required to permit the development of the boundary layer. A 75 wt% glycerol solution requires the greatest hydrodynamic entrance length, of 20 cm, as a result of its relatively low viscosity and high density. This is in agreement with the experimental design since the circular sensor arrays are located 41 cm from the closest potential flow disturbance. Therefore, the assumption of fully developed laminar flow can be discounted affording laminar flow theory and constitutive rheological models to be applied across all of the performed experiments. Additionally, the PIV flow field is axisymmetric; this is an additional assumption which may now be removed.

Not only are the assumptions able to be removed, but the shape and magnitude of the radially averaged velocity mimic the velocity profiles obtained by electrical resistance sensing. A correlation coefficient, R^2, of 0.99 exists between the ERR and PIV glycerol velocity profiles with a root mean squared error (RMSE) of just 0.0064 m s^{-1}. Therefore, the independent velocity profile measurements displaying excellent agreement with ERR for the Newtonian glycerol solution.

Excellent agreement is also observed when the rheology of the process media is changed, Figure 6b. The blunted velocity profile of the yield stress fluid, 1.0 wt% Carbopol, pH 7, is obtained in both the PIV and ERR measurements. A similar comparison as conducted for glycerol may be performed with an outputted RMSE of 0.0048 m s^{-1}, 2.8 % of the average velocity, and correlation coefficient of 0.99.

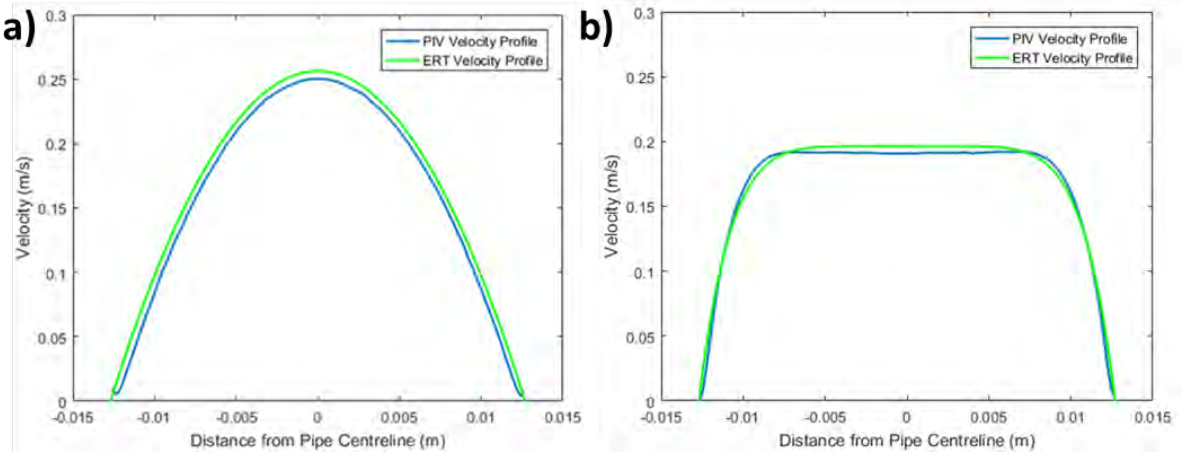

Figure 6. PIV Cross-Sectional Velocity Profile: (a) comparison of the radially averaged PIV glycerol velocity profile and average ERR velocity profile; (b) comparison of the radially averaged PIV Carbopol velocity profile and average ERR velocity profile (Machin et al, 2018)

Despite this experiment being conducted without the presence of the ohmic heater, the acquired velocity profiles obtained from both PIV and ERR are analogous. Accordingly, it may be deemed that the thermal energy dissipation has a negligible impact upon the flow. The similarity between the comprehensive PIV measurement, theoretical laminar velocity profiles and Electrical Resistance Tomography is a significant validation of this novel in-line velocity profile measurement technique.

The velocity profile may be utilised unaccompanied as a fingerprinting in-line rheometer in the case of rheologically complex fluids which do not adhere to constitutive equations. This study has also verified the electrical field penetration of the multi-scale arrays velocity vectors within the conductivity range of 1-9 mS cm^{-1}. This is a similar conductivity range to the experiments performed in Section 5.1.

5.4 Rheology

The rheological parameters determined by ERR have also been compared to off-line, rotational rheometry in Table 1. In the measurement of accuracy, the rheological parameters outputted by the rotational rheometer may be considered as the ‘true’ value; however, it is known that a direct comparison of the two rheometry techniques is imperfect as ERR affords a characterisation within the flow environment. This is unable to be captured using conventional methods.

Using ERR, the mean obtained viscosities for aqueous 75 wt%, 85 wt% and 92.5 wt% glycerol solutions were 0.0223 Pa s, 0.0982 Pa s and 0.250 Pa s, respectively. With the requirement of a single parameter being extracted, the viscosity of a Newtonian fluid is able to be achieved with excellent reliability with the 95 % confidence interval approximately 2.5 % of the mean value. In addition to repeatability, the measured viscosity displays good agreement with the rotational rheometer with an average accuracy of 99.1 %. Therefore, the rheological parameters obtained by off-line rheometers is analogous to that of ERR in the case of simple fluids. Accordingly, it can be said that ERR is able to act as an in-line viscometer.

Table 1. A comparison of an off-line rotational Rheometer with the Electrical Resistance Rheometer. Note: The uncertainty represented within this Table is the 95% confidence interval of the fitted parameters (Machin et al, 2018)

Material	TA R2 Rotational Rheometer μ, Pa s	Electrical Resistance Rheometer μ, Pa s
75 wt% Glycerol	0.0226 (R^2=0.9997)	0.0223 ± 0.0004 (R^2 = 0.994)
85 wt% Glycerol	0.0986 (R^2=0.9993)	0.0982 ± 0.003 (R^2 = 0.995)
92.5 wt% Glycerol	0.254 (R^2=0.9993)	0.250 ± 0.004 (R^2 = 0.992)

	τ_y, Pa	k, Pa s^n	n	τ_y, Pa	k, Pa s^n	n
0.1 wt% XG		0.0712	0.723 (R^2 = 0.99)		0.0740 ± 0.003	0.704 ± 0.04 (R^2 = 0.99)
0.5 wt% XG		1.27	0.350 (R^2 = 0.991)		1.21 ± 0.04	0.348 ± 0.02 (R^2 = 0.99)
1.0 wt% XG		6.13	0.195 (R^2 = 0.995)		6.18 ± 0.2	0.197 ± 0.01 (R^2 = 0.993)
0.1 wt% Carbopol	0.350	0.342	0.604 (R^2 = 0.999)	0.32 ± 0.02	0.372 ± 0.02	0.601 ± 0.04 (R^2 = 0.99)
1.0 wt% Carbopol	29.7	5.93	0.460 (R^2 = 0.991)	29.1 ± 1.7	5.80 ± 0.3	0.486 ± 0.04 (R^2 = 0.994)

As the complexity of the selected constitutive model increases, a simple univariate model validation beomces inadequate. The parameter estimation becomes ill-conditioned; the constitutive models may be described by two or more parameters with the analysis performed from a single velocity profile (Stitt et al, 2015). The power law behaviour of xanthan gum is described by both the consistency index and power index, and hence poses an ill-conditioned problem; however, the incorporation of the Levenberg-Marquadt algorithm has been seen to be vital to dampen the instability in the measurement. Contrary to this, the ERR rheological parameters are seen to mirror those obtained from a conventional rotational rheometer possessing an accuracy of 97.4 % and 98.5 % for k and n, respectively.

As expected, the introduction of a third parameter through the utilisation of the Herschel-Bulkley model produces the greatest variability of the measurement at around ± 6 %. Despite the outputted rheological additionally observing reduced accuracy, when compared to a rotational rheometer, the values obtained from ERR can be seen to be in good agreement. This arises as a consequence of the parametric fitting with the off-line rheometer parameters yielding a theoretical velocity profile which has a correlation coefficient of 0.97 with the ERR velocity profile. This may be reflected as the outputted values from the off-line rheometer lie within the 95 % confidence interval of the ERR rheometry.

Overall, the non-linear least square fitting from the ERR accurately and repeatedly outputs the desirable rheological parameters which mimic conventional rotational rheometry. ERR can therefore be utilised as an effective, robust, in-line rheometer. If the fluids are not known to adhere to conventional rheological models this velocimetry technique may additionally act as a standalone fingerprinting tool for rheology without the requirement of the measurement of differential pressure.

6 CONCLUSIONS

An in-line Electrical Resistance Rheometry (ERR) technique has been presented which utilises a multi-scalar arrangement of non-invasive, microelectrical tomography arrays to elucidate the in-situ rheological behaviour of process fluids. A novel electrical resistance sensor has been developed which consists of two electrode arrangements, linear and circular. The manipulation of the linear array length, and ultimately electrical field penetration, to target sensitivity to the near-wall region and ensure a complete velocity profile was achieved. The ability of multi-scale sensors to target desired regions has also been demonstrated in a COMSOL model of a fluid which has a conductivity of 1 mS cm^{-1}.

ERR is advantageous over conventional off-line techniques as it is able to be directly applied to the process environment and removes the requirement for sampling. This in-line measurement has been achieved utilising the cross-correlation of computed conductivity pixels to tag the motion of a fluid in the pipe to extract a radial velocity profile. The acquired velocity profiles were then validated using the well-established technique of Particle Image Velocimetry, which not only was in excellent agreement, but also validated the assumptions made in the rheological extraction. ERR coupled with the measurement of differential pressure was then additionally was seen to be in excellent agreement with rotational rheometry across a range of fluids described by differing constitutive behaviour. The ERR

multi-scale sensor therefore offers new capabilities of the in-situ analysis of fluids relevant to formulated products with respect to process optimisation, understanding and control. This study is the first in which manipulation of the linear array length, and consequently electrical field penetration, has been utilised this provides an opportunity for the development of a number of multi-scalar electrical resistance sensing techniques in various unit operations for example stirred vessels.

7 ACKNOWLEDGEMENTS

This work was conducted as a part of an EngD project which is financed by the EPSRC Centre for Doctoral Training in Formulation Engineering (EP/L015153/1), Industrial Tomography Systems PLC and the University of Birmingham. All participants of the InnovateUK EMFormR project (EP/L505778/1) are acknowledged for their technical input with special regards to Dr. Tom L. Rodgers, for the use of the University of Manchester, SKID 1 flow loop.

REFERENCES

BLYTHE, T.W; SEDERMAN, A; STITT, E.H; YORK, A; GLADDEN, L, (2017) PFG NMR and Bayesian Analysis to Characterise non-Newtonian Fluids. *Journal of Magnetic Resonance.* 274, 103-114.

DONG, X; TAN, C; DONG, F, (2016) Oil-water two-phase flow measurement with combined ultrasonic transducer and electrical sensors. *Measurement Science and Technology.* 27(12).

KNIRSCH, M; DOS SANTOS, C; DE OLIVEIRA SOARES VICENTE, A; VESSONI PENNA, C, (2010) Ohmic Heating, A Review. *Trends Food Sci.* 21(9), 436-441.

MACHIN, T.D; WEI, K; GREENWOOD, R.W; SIMMONS, M.J.H, (2018) In-pipe Rheology and Mixing Characterisation using Electrical Resistance Sensing. *Chemical Engineering Science.*

MARQUADT, D, (1963) An algorithm for least squares estimation on non-linear parameters. *SIAM J App Maths.* 11, 431-444.

PAPOULIS, A, (1962) *The Fourier Integral and Its Applications.* McGraw-Hill: New York. 244-253.

QIU, C; DICKIN, F.J; JAMES, A.E; WANG, M, (1994). Electrical Resistance Tomography for Imaging sub-seabed sediment porosity: Initial findings from laboratory-scale experiments using spherical glass beads. *Proc. of 3rd European Concerted Action on Process Tomography,* 24-26 March. Oporto. Portugal.

REES, J, (2014) Towards online, continuous monitoring for rheometry of complex fluids. *Advances in Colloid and Interface Science.* 206, 294-302.

REN, Z; KOWALSKI, A; RODGERS, T, (2017) Measuring Inline Velocity Profile of Shampoo by Electrical Resistance Tomography (ERT). *Flow Measurement and Instrumentation.* 58, 31-37.

RIDES, M; JEZEK, J; DERHAM, B; MOORE, J; CERASLOI, E; SIMLER, R; PEREZ-RAMIREZ, (2011) Viscosity of concentrated therapeutic protein compositions. *Advanced Drug Delivery Reviews:* 63(13), 1107-1117

SHARIFI, M; YOUNG, B, (2013) Electrical Resistance Tomography (ERT) for flow and velocity profile measurement of a single phase fluid in a horizontal pipe. *Chemical Engineering Research and Design:* 91 (7), 1235-1244.

SIMMONS, M.J.H; EDWARDS, I; HALL, J.F; FAN, X; PARKER, D.J; STITT, E.H, (2009) Techniques for Visualisation of Cavern Boundaries in Opaque Industrial Systems. *AIChE Journal*. 55(11), 2765-2772.

SMYTHE, W.B, (1968). Static and Dynamic Electricity. Mgraw-Hill: London

STITT, E.H; MARIGO, M; WILKINSON, S; DIXON, T, (2015) How Good is Your Model? *Johnson Matthey Technol. Rev.* 68(2), 74-89.

WANG, M, (2002) Inverse Solutions for Electrical Impedance Tomography Based on Conjugate Gradients Methods. *Measurement Science and Technology*. 13, 101-117.

WANG, M, (2015) Principles of Process Tomography, in Industrial Tomography - Systems and Applications, Elsevier, ISBN: 978-1-78242-118-4.

WILKINSON, W.L, (1960) Non-Newtonian Fluids – Fluid Mechanics, Mixing and Heat Transfer. Pergamon Press Ltd: London, 1-38.

WIKLUND, J; SHAHRAM, I; STADING, M, (2007) Methodology for In-line Rheology by Ultrasound Doppler Velocity Profiling and Pressure Difference Techniques. *Chemical Engineering Science*. 62(1), 4277-4293.